*Journal of Ceramic Processing Research. Vol. 17, No. 7, pp. 690~693 (2016)*

J O U R N A L O F
**Ceramic Processing Research**

# Controlled synthesis and characterization of $BiVO_4$ dendrites via a hydrothermal method

**Yonggang Wang[a,*], Linlin Yang[a], Xiaofeng Wang[a], Yujiang Wang[a] and Gaorong Han[b]**

[a]*Department of Materials Science and Engineering, Luoyang Institute of Science and Technology, Luoyang 471023, PR China*
[b]*State Key Laboratory of Silicon Materials, Department of Materials Science and Engineering, Zhejiang University, Hangzhou 310027, PR China*

**$BiVO_4$ dendrites have been controllably synthesized by a hydrothermal method without any surfactants or templates. The structure and morphology of the obtained $BiVO_4$ dendrites were characterized by X-ray powder diffraction, scanning electron microscope, transmission electron microscopy, and high-resolution transmission electron microscopy. The effect of the pH values, precursors, solution concentrations, reaction temperature, and reaction time on the morphology and structure of the $BiVO_4$ dendrites was systematically studied for the first time. It is found that the morphologies of the obtained $BiVO_4$ crystallites can vary from cubic-like to dendritic shape. The $BiVO_4$ dendrites can be successfully fabricated by the hydrothermal method at 150 °C and pH 7 when $Bi_2(CO_3)_3$ and $NH_4VO_3$ were used as precursors The resultant dendritic structure has four trunks which have ordered branches on the opposite sides of the trunks. A rational mechanism for the oriental growth of the $BiVO_4$ dendrites is discussed. The preparation of $BiVO_4$ dendrites with well-dened shapes may open new opportunities for wide applications of future nanodevices.**

***Key words*: Hydrothermal, Synthesis, $BiVO_4$ dendrites.**

## Introduction

Recently, bismuth vanadate has aroused much interest due to its unique physical and chemical properties such as ion conductivity, ferroelasticity, and photocatalytic activity under visible-light irradiation [1-4]. However, these technological properties are greatly dependent on their crystal structure, particle morphology, surface area, and particle size. Therefore, much effort has been devoted to the morphology-controlled synthesis of $BiVO_4$ crystals. Up to now, $BiVO_4$ crystals with different morphologies have been successfully prepared, such as nanoparticles [5-9], nanoplates [10-11], microspheres [12-13], decahedral structure [14], nanoplatelets [15], porous particles [16], hollow shells [17], and nanoribbons [18]. However, morphology-controlled synthesis is still a significant step toward realization of functional nanodevices and represents a significant challenge in the field of nanoscale science [19]. In our previous work, we have reported the shape-controlled synthesis of $CaWO_4$ nanocrystals by a simple sonochemical method [20]. In this paper, we report the controlled synthesis of $BiVO_4$ dendrites by a hydrothermal method without any templates or surfactants. The effect of pH value, precursor, solution concentration, reaction temperature, and reaction time on the morphology and structure of $BiVO_4$ dendrites were systematically investigated for the first time. The controlled synthesis of $BiVO_4$ dendritic structures may open new opportunities for wide applications of future nanodevices.

*Corresponding author:
Tel : +86-0379-65928196
Fax: +86-0379-65928196
E-mail: wangyg968@163.com

## Experimental

All the chemicals were analytical grade purity. In a typical experiment, $NH_4VO_3$ and $Bi(NO_3)_3$ were used as the starting materials. Firstly, 0.002 mol $NH_4VO_3$ and 0.002 mol $Bi(NO_3)_3$ were separately dissolved in distilled water and diluted $HNO_3$ to form aqueous solutions. Next, KOH solution was slowly added into the $Bi(NO_3)_3$ solution to precipitate $Bi^{3+}$ ions by constant stirring and $Bi(OH)_3$ precipitate was formed. Then, $NH_4VO_3$ solution was added into the above precipitate solution. The pH of the mixed solution in the autoclave was adjusted to 7 and 14, respectively. Finally, the mixed solution was transferred into the 50ml stainless-steel autoclave for a hydrothermal treatment. The autoclave was sealed, heated and held for some time, and then cooled to room temperature naturally. The resultant precipitates were centrifuged, washed with distilled water, and dried naturally for characterization. The effect of precursor on the formation of $BiVO_4$ was investigated. A contrast experiment was conducted, in which $K_2CO_3$ solution was added into $Bi(NO_3)_3$ solution to get $Bi_2(CO_3)_3$ precursor and other reaction conditions were unchanged.

X-ray diffraction was performed on an X-ray diffractometer (D8 Focus, Germany) using CuKα

radiation. Scanning electron microscope (SEM) images were obtained from SIRION field-emission scanning electron microscope. Transmission electron microscope (TEM) images were taken with a JEOL, JEM-2100 by using an acceleration voltage of 200 kV.

## Results and Discussion

The reaction temperature and pH value signicantly inuence the crystal structures of the obtained products. As displayed in Fig. 1(a), a mixture of monoclinic scheelite and tetragonal zircon $BiVO_4$ was obtained by the hydrothermal method at 150 °C at pH7. When the reaction temperature was increased from 150 °C to 180 °C at pH7 (Fig. 1(b)), the obtained products were a mixture of monoclinic scheelite and tetragonal zircon $BiVO_4$, as well as traces of $Bi_2O_3$. In addition, when the pH value was increased from 7 to 14, neither monoclinic scheelit nor tetragonal zircon $BiVO_4$ could be synthesized by the present hydrothermal route (Figs. 1(c) and 1(d)).

The effect of precursors on the formation of $BiVO_4$ was investigated. A contrast experiment was conducted, in which $Bi(OH)_3$ was replaced by an equimolar amount of $Bi_2(CO_3)_3$ and other reaction conditions were unchanged. As depicted in Fig. 2(a), the diffraction peaks could be indexed to single-phase monoclinic $BiVO_4$ (JCPDS No. 83-1700), indicating that pure monoclinic $BiVO_4$ can be fabricated using $Bi_2(CO_3)_3$ and $NH_4VO_3$ as precursor by the hydrothermal method at 150°C at pH7. However, when the reaction temperature was increased from 150 °C to 180 °C, besides the monoclinic $BiVO_4$, traces of tetragonal zircon $BiVO_4$ were also detected (Fig. 2(b)). It is worth pointing out that the pH value played an important role in the formation of $BiVO_4$. When the pH value was increased from pH7 to pH14, as illustrated in Figs. 2(c) and 2(d), neither monoclinic scheelit nor tetragonal zircon $BiVO_4$ was formed by the hydrothermal route. The SEM image of Fig. 3(a) indicates that the obtained $BiVO_4$ samples consist of a majority of such dendritic nanostructures, revealing the high yield and favorable uniformity achieved by the hydrothermal method using $Bi_2(CO_3)_3$ and $NH_4VO_3$ as precursors at pH7 at 150 °C. A higher magnification TEM image of a single dendrite is illustrated

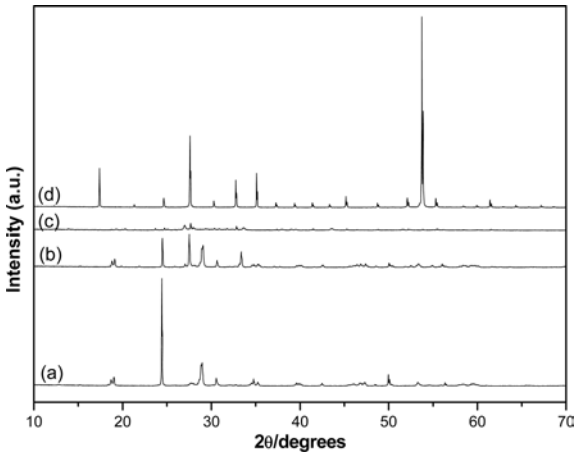


**Fig. 1.** XRD patterns of the samples prepared under different hydrothermal conditions using $Bi(OH)_3$ and $NH_4VO_3$ as precursors for 3 hrs: (a) 150 °C at pH7, (b) 180 °C at pH7, (c) 150 °C at pH14, (d) 180 °C at pH14.

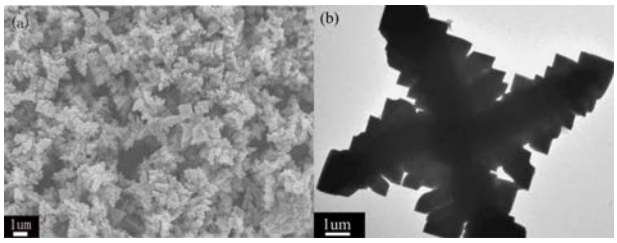


**Fig. 3.** (a) SEM image of the obtained BiVO4 dendrites prepared by the hydrothermal method using $Bi_2(CO_3)_3$ and $NH_4VO_3$ as precursors at pH7 at 150 °C, (b) a typical TEM image of the obtained $BiVO_4$ dendrite.

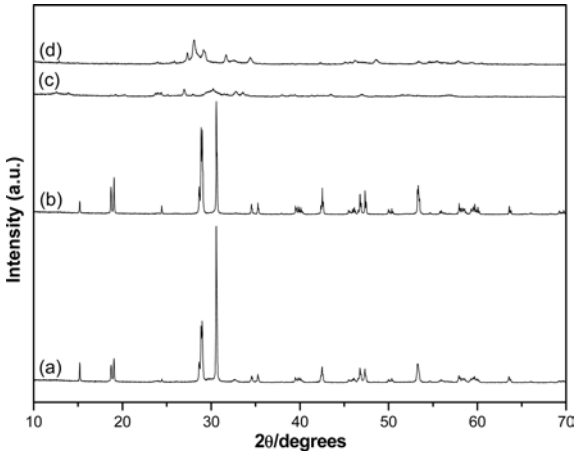


**Fig. 2.** XRD patterns of the samples prepared under different hydrothermal conditions using $Bi_2(CO_3)_3$ and $NH_4VO_3$ as precursors for 3hrs: (a) 150 °C at pH7, (b) 180 °C at pH7, (c) 150 °C at pH14, (d) 180 °C at pH14.

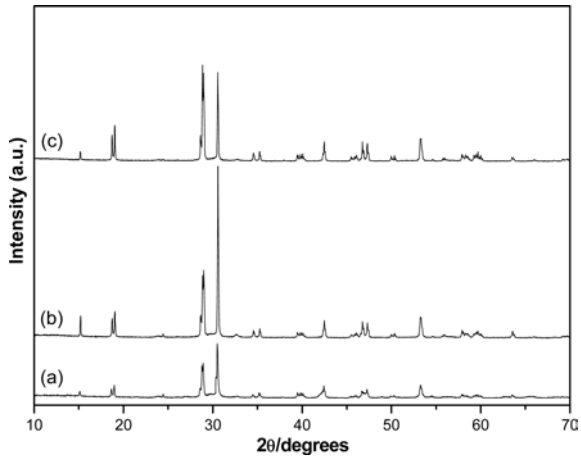


**Fig. 4.** XRD patterns of the samples prepared by the hydrothermal method at 150 °C and pH7 by using $Bi_2(CO_3)_3$ and $NH_4VO_3$ as precursors under different solution concentrations: (a) 0.025 M, (b) 0.05 M, (c) 0.1 M, respectively.

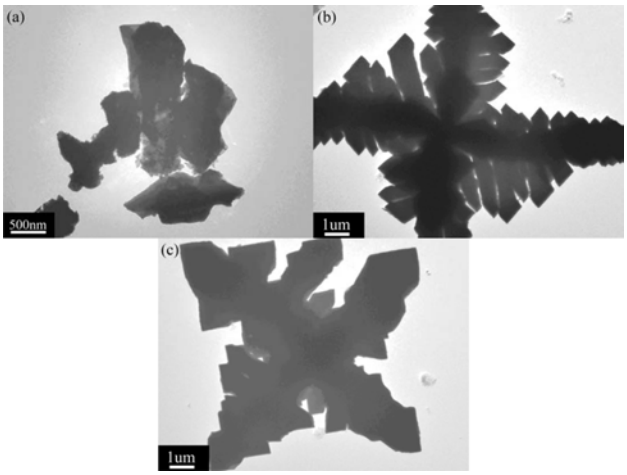


**Fig. 5.** TEM images of the $BiVO_4$ samples prepared by the hydrothermal method at 150 °C and pH7 using $Bi_2(CO_3)_3$ and $NH_4VO_3$ as precursors under different solution concentrations: (a) 0.025M, (b) 0.05 M, (c) 0.1 M, respectively.

in Fig. 3(b), which clearly reveals the dendritic structure.

The effect of solution concentration on the formation of $BiVO_4$ was investigated. Fig. 4 illustrates the XRD patterns of the samples prepared by the hydrothermal method at 150 °C and pH7 by using $Bi_2(CO_3)_3$ and $NH_4VO_3$ as precursors under different solution concentrations. When the concentration increased from 0.025 M to 0.05 M and 0.1 M, all the diffraction peaks can be indexed to monoclinic $BiVO_4$, well consistent with the reported data (JCPDS No. 83-1700). Unreacted or additional phases are not detected.

Figs. 5(a-c) show the corresponding TEM micrographs of the $BiVO_4$ samples prepared by the sonochemical process at 150°C under different solution concentrations. When the concentration was as low as 0.025 M, particles with irregular shapes were obtained (Fig. 5(a)). However, when the concentration was increased to 0.05 M and 0.1 M, respectively, $BiVO_4$ dendrites were formed (Figs. 5(b) and 5(c)). The dendritic structure has four trunks which have ordered branches on the opposite sides of the trunks. The length of the trunks is 5-7 μm while the length of the branches ranges from 500 nm to 2 μm.

A detailed time course study is expected to provide direct evidence of the $BiVO_4$ dendrite formation process. Fig. 6 displays the TEM images of $BiVO_4$ samples obtained by the hydrothermal method at 150°C and pH7 for different reaction times. From Fig. 6(a), it can be observed that cubic-like shaped $BiVO_4$ particles were

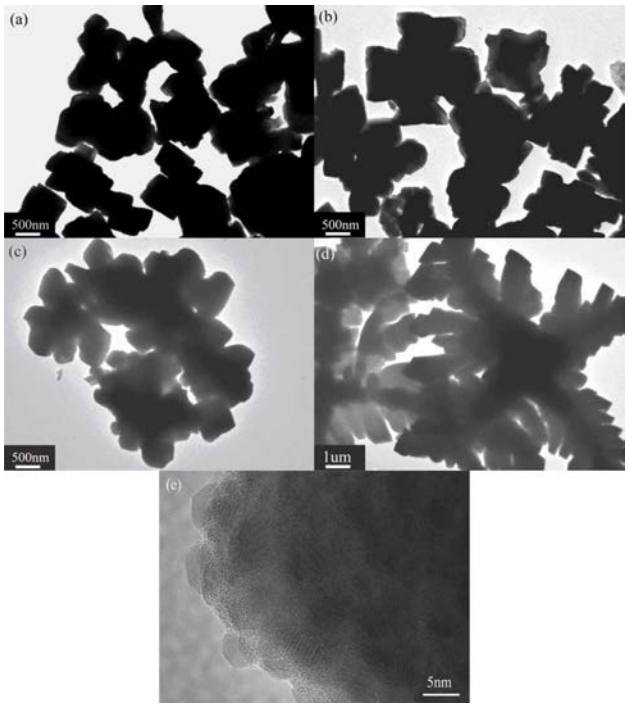


**Fig. 6.** TEM images of the $BiVO_4$ samples prepared by the hydrothermal method at 150 °C and pH7 using $Bi_2(CO_3)_3$ and $NH_4VO_3$ as precursors for different reaction times: (a) 30 min, (b) 1hr, (c) 2 hrs and (d) 3 hrs, respectively. (e) HRTEM image performed on the edge of as-prepared $BiVO_4$ dendrite.

first formed in the case of 30 min. When the reaction time was prolonged to 1hr, the emergence of protrudent corners on the cubic-like particle was observed, indicating the tendency of orientation growth (Fig. 6(b)). As the reaction time was increased to 2 hrs, the protrudent corners obvious grew up (Fig. 6(c)). When the reaction time was further protracted to 3hrs, $BiVO_4$ dendrites were finally formed, as displayed in Fig. 6(d).

The surface morphology of crystals is dependent on the deviation degree of synthetic condition from equilibrium [21]. Crystals generally have simple shapes in the case of equilibrium. However, dendritic growth can be realized when the synthetic condition is driven farther from equilibrium [22]. In the present experiment, when the solution concentration is as low as 0.025 M, the system may be near equilibrium. Therefore, $BiVO_4$ particles with simple shapes were obtained (Fig. 5(a)). However, when the solution concentration was increased to 0.05 M and 0.1 M, the system may be farther from equilibrium, resulting in the formation of $BiVO_4$ dendrites (Figs. 5(b)

**Fig. 7.** Schematic representation of the growing process of $BiVO_4$ dendritic structures.

and 5(c)). The growth process may be explained by the orientated attachment mechanism [23]. We consider that the dendrites are grown from small primary nanoparticles through an orientated attachment process, in which the nanoparticles are self-assembled by sharing a common crystallographic orientation. Fig. 6(e) displays the HR-TEM image of the edge of the obtained $BiVO_4$ dendrites. It can be clearly observed that some small nanoparticles are attached on the dendrite, suggesting the presence of the oriented attachment. Based on the morphology evolution (Figs. 6(a-d)), the growth process of $BiVO_4$ dendrites by the hydrothermal process is described in Fig. 7. As the formation mechanism and hydrothermal conditions are complicated, the exact reason for the formation of $BiVO_4$ dendrites needs to be further studied.

## Conclusions

In summary, $BiVO_4$ dendrites have been successfully fabricated by a hydrothermal process without any surfactants or templates. The morphology and crystal structure of $BiVO_4$ dendrites can be controlled through adjusting the synthetic parameters, such as pH value, precursor, solution concentration, reaction temperature, and reaction time. The preparation of $BiVO_4$ dendrites with well-dened shapes may open new opportunities for wide applications of future nanodevices.

## Acknowledgments

This work is supported by the Natural Foundation of the Education Department of Henan Province (2011B430019) and the Doctor Foundation of Luoyang Institute of Science and Technology (2009BZ05).

## References

1. W. Liu, Y.Q. Yu, L.X. Cao, G. Su, X.Y. Liu, L. Zhang and Y.G. Wang, J Hazard Mater. 181 (2010) 1102-1108.
2. X. Zhang, Z.H. Ai, F.L. Jia, L.Z. Zhang, X.X. Fan and Z.G. Zou, Mater. Chem. Phys. 103 (2007) 162-167.
3. T. Lu and B.C.H. Steele, Solid State Ionics 21 (1986) 339-342.
4. K. Hirota, G. Komatsu, M. Yamashita, H. Takemura, O. Yamaguchi, Mater. Res. Bull. 27 (1992) 823-830.
5. M. Wang, Q. Liu, Y.S. Che, L.F. Zhang and D. Zhang, J. Alloys Compd. 548 (2013) 70-76.
6. R. Venkatesan, S. Velumani and A. Kassiba, Mater. Chem. Phys. 135 (2012) 842-848.
7. C. Karunakaran, S. Kalaivani and P. Vinayagamoorthy, Mater. Lett. 122 (2014) 21-24.
8. B.X. Lei, L.L. Zeng, P. Zhang, Z.F. Sun, W. Sun and X.X. Zhang, Advanced Powder Technology 25[3] (2014) 946-951.
9. U.M. García-Pérez, A. Martínez-de la Cruz, S. Sepúlveda-Guzmán and J. Peral, Ceram. Inter. 40[3] (2014) 4631-4638.
10. X. Meng, L. Zhang, H. Dai, Z. Zhao, R. Zhang, Y. Liu, Mater. Chem. Phys. 125 (2011) 59-65.
11. G.Q. Tan, L.L. Zhang, H.J. Ren, J. Huang, W. Yang and A. Xia, Ceram. Inter. 40[7] (2014) 9541-9547.
12. Y. Liu, J.F. Ma, Z.S. Liu, C.H. Dai, Z.W. Song, Y. Sun, J.R. Fang and J.G. Zhao, Ceram. Inter. 36 (2010) 2073-2077.
13. Z.F. Zhu, J. Du, J.Q. Li, Y.L. Zhang and D.G. Liu, Ceram. Inter. 38[6] (2012) 4827-4834.
14. Z.F. Zhu, L. Zhang, J.Q. Li, J. Du, Y.B. Zhang and J.Q. Zhou, Ceram. Inter. 39[7] (2013)7461-7465.
15. D. Ressnig, R. Kontic and G.R. Patzke, Mater. Chem. Phys. 135 (2012) 457-466.
16. H.Y. Jiang, H.X. Dai, X. Meng, K.M. Ji, L. Zhang and J.G. Deng, Appl. Catal. B: Environ. 105 (2011) 326-334.
17. S.S. Dunkle, R.J. Helmich and K.S. Suslick, J. Phys. Chem. C. 113 (2009) 11980-11983.
18. F.X. Wang, M.W. Shao, L. Cheng, J. Hua and X.W. Wei, Mater. Res. Bull. 44 (2009) 1687-1691.
19. H.Q. Yan, R.R. He, J. Johnson, M. Law, R.J. Saykally and P.D. Yang, J. Am. Chem. Soc., 125 (2003) 4728-4729.
20. L.L. Yang, Y.G. Wang, Y.J. Wang, X.F. Wang and G.R. Han, Advanced Powder Technology 24 (2013) 721-726.
21. Y. Oaki and H. Imai., Cryst. Growth. Des. 3 (2003) 711-716.
22. C.M. Lopez and K.S. Choi., Langmuir. 22 (2006) 10625-10629.
23. J.F. Banfield, S.A. Welch, H.Z. Zhang, T.T. Ebert and R.L. Penn, Science 289 (2000) 751-754.